III. Numerical Results

Letting the lower half-space be perfectly conducting, the correction fact, Δ, is plotted in Figs. 2 and 3 as a function of H for various values of D_1 when $\theta_0 = 0$ and 45°, respectively; the results are in general agreement with those sketched in an earlier study [1]. As expected, the values of Δ for $H \to \infty$ approach those results furnished by MacFarlane [4] where he assumed the grid was located in free space.

Similar results are shown in Figs. 4 and 5 when $N = 1.57$. Fig. 6 shows the correction factor when region 1 is the denser medium (i.e., $N = 1/1.57$) and $\theta_0 = 0$. The general shapes of the curves shown in Figs. 4, 5, and 6 are predicted by (9), and the values of Δ for $H \to \infty$ approach those of MacFarlane. The numerical data in Fig. 6 supersede and extend an earlier investigation [2].

IV. Concluding Remarks

We have extended and updated various results for the correction term used in computing the impedance of a wire grid parallel to a dielectric interface. We stress that the results herein are restricted to the case where the electric field is always parallel to the grid's wires.

References

[1] J. R Wait, "Reflection from a wire grid parallel to a conducting plane," *Can J Phys.*, vol. 32, pp 571–579, Sept 1954.

[2] J. R. Wait, "The impedance of a wire grid parallel to a dielectric interface," *IRE Trans Microwave Theory Tech*, vol. MTT-5, no. 2, pp. 99–102, Apr 1957.

[3] J R Wait, *Introduction to Antennas and Propagation*. London Peregrinus, 1986, ch. 7.

[4] G. G. MacFarlane, "Surface impedance of an infinite parallel-wire grid at oblique angles of incidence," *J. IEE*, vol. 93 (III A), pp. 1523–1527, Dec 1946

Analysis of Wide Transverse Inductive Metal Strips in a Rectangular Waveguide

BRIGHT H. CHU AND KAI CHANG, SENIOR MEMBER, IEEE

Abstract **—An analysis based on the variational method and the moment method has been developed to calculate the discontinuity susceptance due to one or more inductive strips in a rectangular waveguide. The strips can have wide widths and be located unsymmetrically on the transverse plane of the waveguide. The current distribution on the strips has been determined by solving a set of linear equations. The theoretical results agree closely with experiments.**

I. Introduction

Waveguide inductive strip discontinuities have many applications in waveguide filters and matching networks. Many analyses have been reported for single and multiple inductive strips in waveguide [1]–[7]. Marcuvitz provided closed-form formulas for the reactance of a transverse inductive strip with a broad range of widths [1]. The solution is only valid for a centered strip and only one strip can be considered. For a narrow strip, a solution based on the variational method can be found in Collin [2]. The strip location is not limited to the center of the waveguide. Chang and Khan [3], [4] reported an analysis for a two- and a three-strip discontinuity using the variational method. The current density ratios between the strips have also been determined. The analysis is limited to narrow strips since a constant current distribution is assumed on each strip. Furthermore, as the number of strips increases, the analysis becomes very complicated and a large number of nonlinear equations for current ratios are difficult to solve. Lewin reported a method of solving a general unsymmetrical multiple-strip geometry by using a singular-integral equation over a multiple interval [5], [6]. The method was based on the singular-integral equation approach which had previously been applied to a symmetrical double inductive aperture [7]. The analysis is quite general but no numerical results were reported.

The moment method has recently been used for the analysis of a probe-excited waveguide [8] and a single inductive metal post [9]. Analyses for inductive posts and diaphragms have also been reported [10], [11].

This paper reports an analysis based on variational and moment methods to calculate the discontinuity susceptance due to both a single strip and multiple strips in waveguide. The strips are located unsymmetrically on the transverse plane of a waveguide and the widths of the strips can be large. The current distribution on each strip is approximated by pulse expansion functions. The moment method is first used to determine the amplitudes of these expansion functions by solving an integral equation. Once the current distribution is determined, the variational method is used to calculate the discontinuity susceptance. Analyses for both single and multiple strips are given. Theoretical results have been compared with experiments for single wide centered strips, a single wide off-centered strip, a two-strip obstacle, and a three-strip discontinuity. The agreement is very good.

II. Analysis of a Single Wide Strip

It is assumed that the transverse metal strip is located at $z = 0$, as shown in Fig. 1. The strip is assumed to be infinitesimally thin and made of perfect conductor. By the requirement that the tangential E field vanish on the perfectly conducting strip surface S, we have [2]

$$\sin\frac{\pi x}{a} - \frac{j\omega\mu_0}{a}\sum_{n=1}^{\infty}\frac{1}{\Gamma_n}\sin\frac{n\pi x}{a}\int_S \sin\frac{n\pi x'}{a}J(x')\,dx' = 0 \quad (1)$$

where $J(x')$ is the current distribution on the strip, a is the width of the rectangular waveguide, and the integration is performed on the strip surface S. The propagation constant Γ_n is defined as

$$\Gamma_n = \frac{\pi}{a}\sqrt{n^2 - (2a/\lambda_0)^2}.$$

To solve the unknown current $J(x)$, it can be expressed in terms of pulse expansion functions as

$$J(x) = \sum_{q=1}^{N} I_q f(x_q) = \sum_{q=1}^{N} I_q\left[U(x - x_q) - U(x - x_{q+1})\right] \quad (2)$$

where N is the total number of segments for the pulse expansion function, $U(x)$ is the step function, and I_q is the amplitude. The index q indicates the qth segment along the strip. Equation (1)

Manuscript received December 2, 1988; revised February 27, 1989. This work was supported in part by the Texas Higher Education Coordinating Board Advanced Research Program and the Army Research Office

The authors are with the Department of Electrical Engineering, Texas A&M University, College Station, TX 77843-3128.

IEEE Log Number 8927791.

0018-9480/89/0700-1138$01.00 ©1989 IEEE

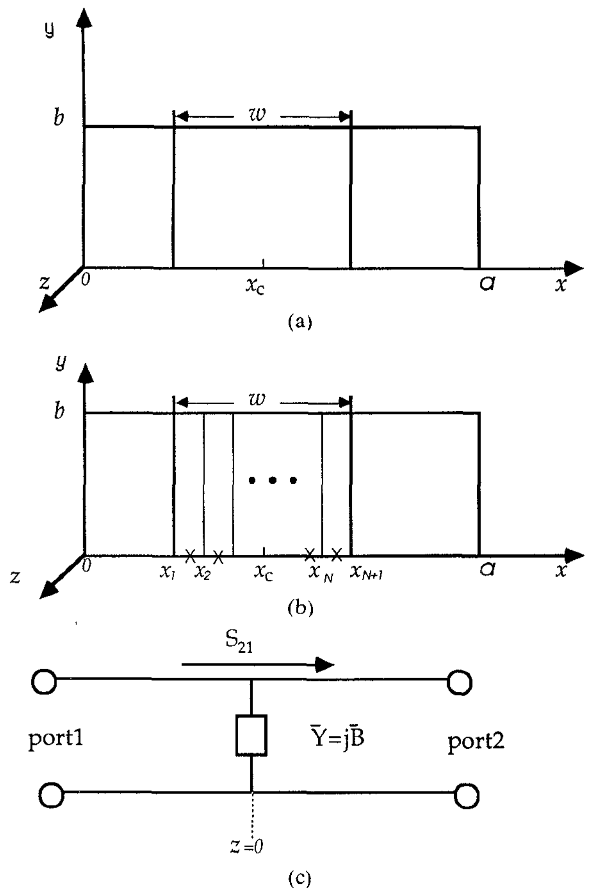

Fig. 1 A rectangular waveguide with a transverse inductive strip. (a) Cross section. (b) Pulse expansion function with matched points indicated by crosses. (c) Equivalent circuit.

becomes

$$\sum_{q=1}^{N} I_q \sum_{n=1}^{\infty} \frac{1}{\sqrt{n^2-(2a/\lambda_0)^2}} \left[\sin\frac{n\pi(x+x_q)}{a} + \sin\frac{n\pi(x-x_q)}{a} - \sin\frac{n\pi(x+x_{q+1})}{a} - \sin\frac{n\pi(x-x_{q+1})}{a} \right] = -\frac{j\pi}{c\mu_0(a/\lambda_0)} \sin\frac{\pi x}{a} \quad (3)$$

where c is the speed of light.

The coordinates of the locations of the segments can be calculated as follows:

$$x_q = x_c - \frac{w}{2} + (q-1)h \quad (4)$$

where x_c is the center location of the strip, w is the width of the strip, and h is w/N.

By choosing a suitable weighting function, (3) can be converted to a system of linear equations of amplitudes I_q, $q=1,2,\cdots,N$. The dimensions of the system of linear equations are N by N if the following procedure is adopted. The procedure is to multiply both sides of (3) by the weighting functions and then integrate both sides. The type of weighting functions is chosen to be

$$W(\bar{x}_p) = \delta(x-\bar{x}_p), \qquad p=1,2,\cdots,N \quad (5)$$

where $\bar{x}_p = (x_p + x_{p+1})/2$ are the matched points located at the centers of segments. This is the matched-point method and the weighting functions are of the impulse function type. Although this is the simplest type of weighting function, the results are very good, as shown in the following sections. The locations of the segments, together with the matched points, are illustrated in Fig. 1(b).

The calculated current can be utilized in the following variational formula to obtain the normalized susceptance [2]:

$$\bar{B} = \frac{B}{Y_0} = -\frac{2j}{\Gamma_1} \frac{\left| \int_S J(x) \sin\frac{\pi x}{a}\, dx \right|^2}{\sum_{n=2}^{\infty} \frac{1}{\Gamma_n} \int_S \int_S J^*(x) J(x') \sin\frac{n\pi x}{a} \sin\frac{n\pi x'}{a}\, dx\, dx'}. \quad (6)$$

For the pulse expansion function, the variational formula becomes

$$\frac{B}{Y_0} = -\frac{2j}{\Gamma_1} \frac{\left| \sum_{q=1}^{N} I_q \left(\cos\frac{\pi x_q}{a} - \cos\frac{\pi x_{q+1}}{a} \right) \right|^2}{\sum_{n=2}^{\infty} \frac{1}{n^2 \Gamma_n} \left| \sum_{q=1}^{N} I_q \left(\cos\frac{n\pi x_q}{a} - \cos\frac{n\pi x_{q+1}}{a} \right) \right|^2}. \quad (7)$$

The infinite series are truncated after n_T terms determined by a method presented by Eisenhart and Khan [12]. The truncation will save computation time without loss of accuracy.

III. Results for Single Strips

Measurements were carried out with strips in a conventional X-band rectangular waveguide with a width of 0.9 in and a height of 0.4 in. The strip is made of copper with a thickness 0.005 in. An HP8510 network analyzer was used to measure the S_{21} parameter. From the S_{21} parameter, the discontinuity susceptance can be calculated. Since the strip is assumed to be lossless, it can be represented by the circuit shown in Fig. 1(c) with matched circuits on both sides. We have

$$S_{21} = |S_{21}| e^{j\phi} = \frac{2}{2+\bar{Y}}.$$

The normalized susceptance can be found as follows:

$$\bar{B} = \frac{B}{Y_0} = -\frac{2\sin\phi}{|S_{21}|}. \quad (8)$$

A. Single Centered Strips

Experiments were performed for strips with widths of $w = 0.118$ in ($0.131a$), 0.276 in ($0.306a$), 0.433 in ($0.481a$), and 0.472 in ($0.525a$). The number of segments is determined to be 30 per free-space wavelength, i.e., $SNPW = 30$. A comparison between measurements and theoretical results is given in Fig. 2 ($f =$ 9 GHz or $a/\lambda_0 = 0.6858$) as a function of strip width. It can be seen that the theoretical results agree closely with measurements. A comparison between the theoretical results and Marcuvitz's formula is also shown in Fig. 2. From these curves, it can be seen that the absolute value of the susceptance is increased as the width of the strip increases.

Computational studies have been carried out to determine the number of segments required for calculation. The selection of 30 segments was based on the fact that little improvement in accuracy can be obtained for more than 30 segments. However, loss of accuracy could occur when the number of segments is less than 30.

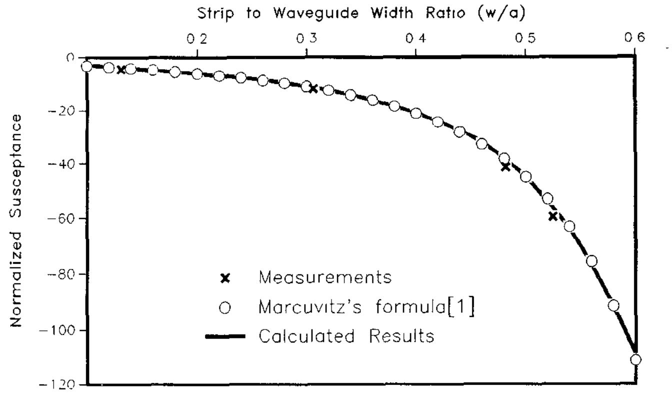

Fig. 2. Calculated normalized susceptance versus measurements and Marcuvitz's results at 9.0 GHz for centered strips.

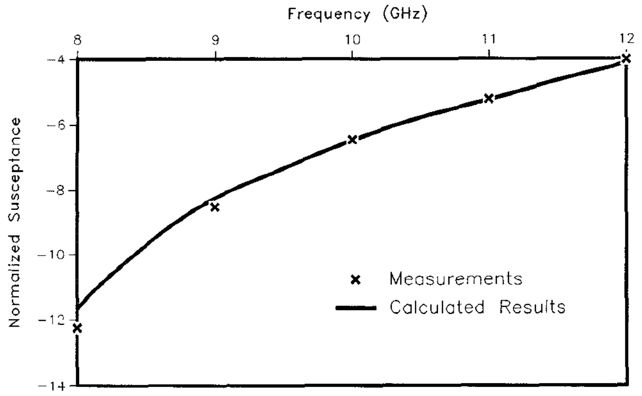

Fig 3 Normalized discontinuity susceptance as a function of frequency for a strip centered at 0 416a with a width of 0 276 in.

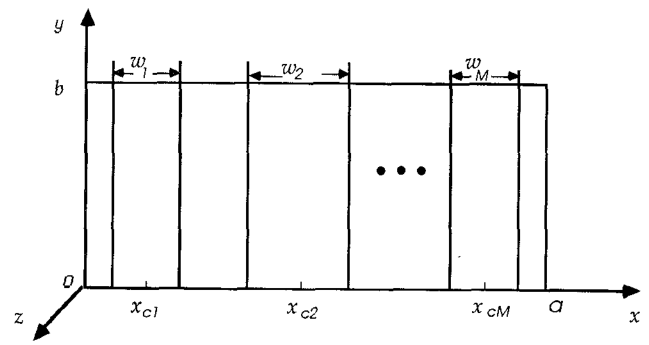

Fig. 4 Cross section of rectangular waveguide with M transverse inductive strips.

B. Single Off-Centered Strips

Measurements for off-centered strips have also been carried out for a strip centered at 0.375 in (0.416a) with a width of 0.276 in (0.306a). A comparison between the experimental and the theoretical results is shown in Fig. 3. Again, the agreement is very good.

IV. Results for Two and Three Strips

The analysis given in Section II can be extended to various configurations of multiple strips. The geometry of multiple strips is shown in Fig. 4.

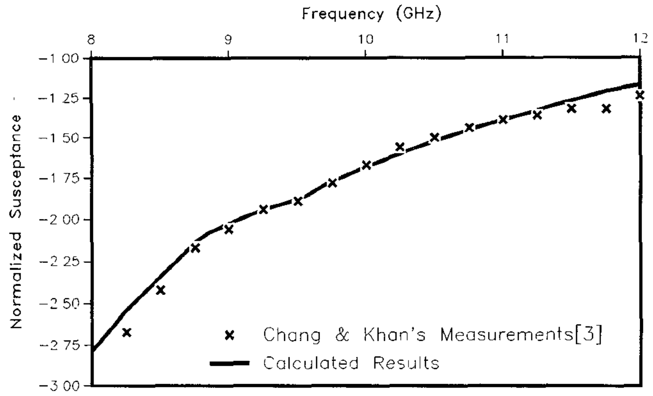

Fig 5 Calculated normalized susceptance versus measurements for two strips in the case of [3, fig 4(a)].

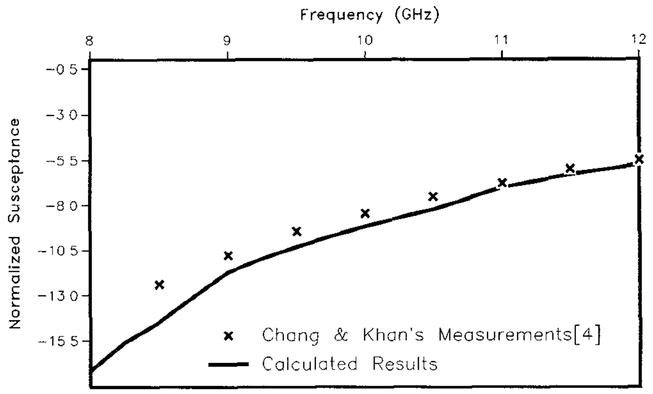

Fig. 6. Calculated normalized susceptance versus measurements for three strips in the case of [4, fig 2]

A. Two Strips

The theoretical results using the pulse expansion function were compared with Chang and Khan's experiments shown in [3, fig. 4(a)]. They agree closely, as shown in Fig. 5. To calculate the current ratio, the total current on each strip is the sum of the currents on segments if there is more than one segment on each strip.

B. Three Strips

The theoretical results for a three-strip discontinuity were compared with Chang and Khan's experiments in [4, fig. 2] as shown in Fig. 6. The agreement is fairly good, especially at the high-frequency end. Since the experimental results were obtained by slotted line measurement, the discrepancies at the low-frequency end are believed to be caused by the error in measuring high susceptance.

V. Conclusions

A method to calculate the discontinuity susceptance of transverse inductive strips in a rectangular waveguide has been developed. The method is based on the variational method and moment method for impedance and current calculation. The results compare favorably with Chang and Khan's experimental data [3], [4], Marcuvitz's results [1], and our own experimental measurements. The advantages of this method are that strips can be wide and the locations of the strips are flexible.

Acknowledgment

The authors would like to thank Dr. R. D. Nevels for his encouragement and M. Li for his assistance in measurements.

References

[1] N. Marcuvitz, *Waveguide Handbook.* New York: McGraw Hill, 1951, ch. 5.
[2] R. E. Collin, *Field Theory of Guided Waves.* New York: Mc Graw Hill, 1960, ch. 8.
[3] K. Chang and P. J Khan, "Coupling between narrow transverse inductive strips in waveguides," *IEEE Trans. Microwave Theory Tech.*, vol. MTT-24, pp. 101–105, Feb. 1976.
[4] K. Chang and P. J. Khan, "Analysis of three narrow transverse strips in waveguide," in *1978 MTT-S Int Microwave Symp. Tech Dig.*, pp. 419–421.
[5] L. Lewin, "Solution of a singular integral equation over a multiple interval and applications to multiple strips, grids or waveguide diaphragms," *Electron Lett.*, vol. 2, pp 458–459, Dec. 1966.
[6] L. Lewin, *Theory of Waveguides.* New York: Wiley, 1974, chs. 6 and 7.
[7] L. Lewin, "The use of singular integral equation in the solution of waveguide problems," in *Advances in Microwaves*, vol. 1, L. Young, Ed New York: Academic Press, 1966, pp. 241–247.
[8] J. M. Jarem, "A multifilament method-of-moments solution for the input impedance of a probe-excited semi-infinite waveguide," *IEEE Trans Microwave Theory Tech.*, vol. MTT-35, pp. 14, Jan. 1987.
[9] Y. Leviatan, P G. Li, A T. Adams, and J. Perini, "Single-post inductive obstacles in rectangular waveguide," *IEEE Trans. Microwave Theory Tech.*, vol. MTT-31, pp. 806–811, Oct. 1983.
[10] Y Leviatan and G. S. Sheaffer, "Analysis of inductive dielectric posts in rectangular waveguide," *IEEE Trans. Microwave Theory Tech*, vol. MTT-35, pp. 48–59, Jan 1987.
[11] H Auda and R. F. Harrington, "Inductive posts and diaphragms of arbitrary shape and number in a rectangular waveguide," *IEEE Trans. Microwave Theory Tech.*, vol. MTT-32, pp. 606–613, June 1984.
[12] R. L Eisenhart and P. J. Khan, "Theoretical and experimental analysis of a waveguide mounting structure," *IEEE Trans Microwave Theory Tech.*, vol MTT-19, pp. 706–719, Aug 1971.

On Microwave Imagery Using Bojarski's Identity

TAH-HSIUNG CHU, MEMBER, IEEE, AND DING-BING LIN

***Abstract*—In this paper, theoretical and experimental studies of microwave imagery of a perfectly conducting convex object of a size larger than the incident wavelength are presented. Experimental data were measured in the frequency range 4–10 GHz. Calculations were done with Bojarski's identity, one-dimensional Fourier inversion of the range-normalized scattered far field, and a back-projection algorithm. The images show the distribution of specular reflection regions on the surface of the object.**

I. Introduction

Bojarski's identity [1], [2] forms the basis for imaging a perfectly conducting convex object under physical optics approximations. The identity states that the characteristic function $\gamma(\boldsymbol{r})$ of the object, which is unity inside the scattering object and zero outside, and $\Gamma(\boldsymbol{p}) = 2\sqrt{\pi}p^{-2}[\rho(\boldsymbol{p}) + \rho^*(-\boldsymbol{p})]$ make up a Fourier transform pair where $\boldsymbol{r}$ is a position vector and $\boldsymbol{p} = -2k\hat{i}_k = p\hat{i}_p$, with $\hat{i}_k$ as the direction of the incident plane wave. The quantity $\rho(\boldsymbol{p})/p$ is the range-normalized scattered far field measured at all frequencies and viewing angles. However, in the case of microwave imaging, the reconstructed image becomes the derivative (or the edge information) of the characteristic function, since a band-pass version of $\Gamma(\boldsymbol{p})$ is measured [3], [4]. The image resolution is inversely proportional to the $\boldsymbol{p}$-space aperture (or area of $\Gamma(\boldsymbol{p})$) formed by varying frequency and viewing angle.

Manuscript received August 19, 1987; revised December 19, 1988. This work was supported by the National Science Council of the Republic of China under Grant NSC 77-0404-E002-40
The authors are with the Electrical Engineering Department, National Taiwan University, Taiwan, Republic of China.
IEEE Log Number 8927796.

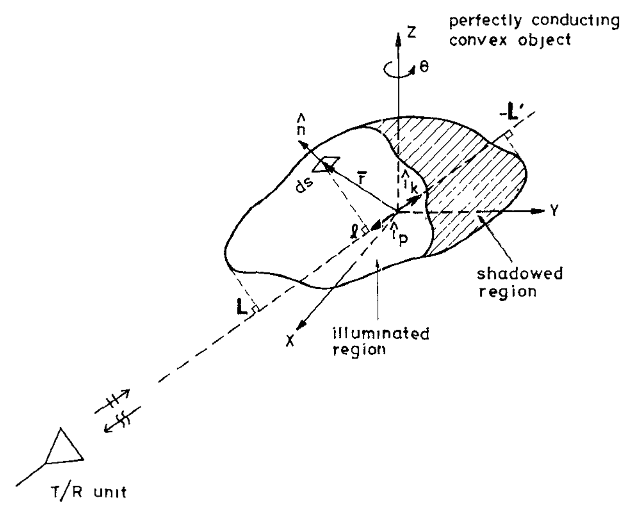

Fig. 1. The scattering geometry

It is known that the far field scattered by a metallic object subjected to coherent microwave illumination is determined by the relative positions of scattering centers on the illuminated portion of the object [5]. A scattering center is defined as the object structure that is observed in the backscattered field. For a smooth convex object of size larger than the incident wavelength, these scattering centers are the specular reflection regions distributed on the illuminated object surface.

The aim of this paper is to show analytically and experimentally that the reconstructed image of a convex metallic object using Bojarski's identity gives the distribution of these specular regions over the entire object surface.

II. Theoretical Analysis

As a perfectly conducting convex object is illuminated with a monochromatic plane wave propagating in the direction $\hat{i}_k$, as shown in Fig. 1, its range-normalized backscattered far field under physical optics approximations can be expressed as [1], [2]

$$\frac{\rho(\boldsymbol{p})}{p} = \frac{j}{2\sqrt{\pi}} \int_{\hat{i}_p \cdot \hat{n} > 0} (\hat{i}_p \cdot \hat{n})\, e^{-j\boldsymbol{p}\cdot\boldsymbol{r}}\, dS(\boldsymbol{r}) \qquad (1)$$

where $\boldsymbol{p} = -2k\hat{i}_k = p\hat{i}_p$, $k = 2\pi f/c$, $\hat{n}$ is the outward vector normal to the object surface $S(\boldsymbol{r})$, and the surface integral is over the illuminated portion of the object. In general, this surface integral cannot be integrated analytically. However, by adding $\rho(\boldsymbol{p})$ with $\rho^*(-\boldsymbol{p})$ measured with the transmitter/receiver (T/R) unit at the other side of the object and using the divergence theorem, one can obtain [1], [2]

$$\Gamma(\boldsymbol{p}) = \frac{2\sqrt{\pi}}{p^2}[\rho(\boldsymbol{p}) + \rho^*(-\boldsymbol{p})] = \int \gamma(\boldsymbol{r})\, e^{-j\boldsymbol{p}\cdot\boldsymbol{r}}\, d\boldsymbol{r} \qquad (2)$$

where $\gamma(\boldsymbol{r})$ is the characteristic function of the scattering object B, defined as

$$\gamma(\boldsymbol{r}) = \begin{cases} 1, & \boldsymbol{r} \text{ in B} \\ 0, & \boldsymbol{r} \text{ not in B.} \end{cases} \qquad (3)$$

Equation (2) is known as Bojarski's identity [1], [2]. It shows that an image of the scattering object B can be reconstructed from the backscattered far field measured at all frequencies and viewing angles through the Fourier inversion. The reconstructed